Ground stability monitoring with pore water pressure and displacement profile measurements

A.B. Huang, J.T. Lee, and Y.T. Ho
Department of Civil Engineering, National Chiao Tung University, Hsinchu, Taiwan
E-mail: huanganbin283@gmail.com

Summary: Over the past few decades, many optical fibre sensing techniques have been developed. Among these available sensing methods, optical fibre Bragg grating (FBG) is probably the most popular one. With its unique capabilities, FBG based geotechnical sensors can be used as a sensor array for distributive (profile) measurements, deployed under water (submersible), for localized high resolution and/or differential measurements. The authors have developed a series of FBG based transducers that include inclination, linear displacement and gauge/differential pore-pressure sensors. Techniques that involve the field deployment of FBG inclination, extension and pore-pressure sensor arrays for automated slope stability and ground subsidence monitoring have been developed. The paper provides a background of FBG and the design concepts behind the FBG based field monitoring sensors. Cases of field monitoring using the FBG sensor arrays are presented, their practical implications are discussed.

1. INTRODUCTION

Most of the existing electrical sensor and cable systems are prone to adverse effects of electro-magnetic inference (EMI), short circuit, and lightning. Fibre optic sensors have features that are especially appealing for geotechnical field monitoring where the sensors are often subject to extreme or harsh conditions. Common drawbacks of the electrical sensors can be significantly and readily avoided when using the fibre optic sensors. Of the many available techniques, the authors have been concentrating on the use of Fibre Bragg Grating (FBG) as a core sensing element in their developments of a series of fibre optic sensored geotechnical field monitoring systems. This paper provides a brief background of FBG, presents the experiences in the application of various FBG sensored monitoring and discusses implication in the use of FBG systems developed by the authors.

2. FBG AS A PARTIALLY DISTRIBUTIVE STRAIN SENSOR

Optical fibres are made of silica, with a diameter about the same of a human hair, and can transmit light over long distances with very little loss of fidelity. Optical fibres comprise two essential components: a core surrounded by an annular cladding. The core of the optical fibre serves to guide light along the length of the optical fibre. The cladding has a slightly lower index of refraction than the core. Its primary function is to ensure total internal reflection within the core and that very little light is lost as it propagates along the core of the optical fibre. The typical combined diameter of core and cladding is 125 μm. The silica core/cladding is protected by an acrylic coating. The total outside diameter of an optical fibre with the acrylic coating is 250 μm. By adopting technologies from telecommunication, many fibre optic based sensing techniques have been developed. The fibre optic Bragg grating (FBG) is one of the many available forms of optical fibre sensors. An FBG is made by a periodic variation of fibre core refractive index. The typical length of an FBG is 1 to 20 mm long. When the FBG is illuminated by a wideband light source, a fraction of the light is reflected back upon interference by the FBG. The wavelength of the reflected light, is linearly related to the longitudinal strains of the FBG (Rao, 1998), thus making FBG an ideal strain gage. The returned signal from every FBG carries a unique domain of wavelength, making it possible to have multiple FBG elements on the same fibre. The multiplexing among various sensors on a single fibre can be accomplished by wavelength division addressing as conceptually described in Figure 1. The FBG is partially distributive because only those parts of the optical fibre with FBG are used as strain sensors and these sensors can share the same optical fibre transmission line.

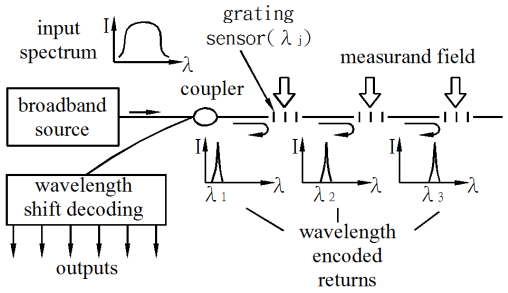

Figure 1 Schematic diagram of Fibre Bragg Grating (adapted from Kersey, 1992), I = light intensity λ = wavelength.

3. FBG SENSORED FIELD MONITORING DEVICES

The FBG can be used directly as a strain gage, or, with the help of mechanical components, FBG can be configured as displacement, pressure and inclination transducers. All advantages of the FBG can be inherited in FBG-based transducers for geotechnical engineering monitoring purposes. These advantages can include: partially distributive, high resolution, good signal stability and immunity to EMI. The FBG based sensors can be used as an individual sensor to reflect the physical quantity at a given location or connected into an array so that the profile of a given or multiple types of physical quantities can be monitored. The following section describes some of FBG the based transducers developed by the authors that relate to ground stability monitoring.

2.1 The FBG-IPI

The FBG sensored, pendulum type in-place inclinometer (FBG In-Place Inclinometer, FBG-IPI) was developed for the purpose of monitoring variations of inclination in reference to gravity. As conceptually depicted in Figure 2, a mass is linked to a hinge. A pair of FBG's are fixed to the sides of the mass. The FBG's pair experiences elongation strains in opposite signs but equal amount, when the mass is rotated away from verticality against the hinge. Thus, the FBG pair senses the amount of rotation and offsets the temperature effects.

2.2 The FBG Pressure Transducer

Figure 3 shows a schematic view and photograph of an FBG pressure transducer. The FBG was used to sense the deflection of a metallic diaphragm inside of the transducer due to changes in pressure against the atmosphere. A separate FBG was placed inside the transducer to monitor temperature fluctuations. The range of pressure transducer was controlled by the stiffness of the diaphragm.

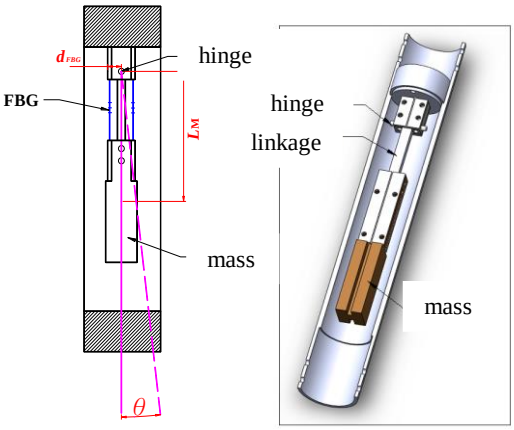

Figure 2 Design of the FBG-IPI.

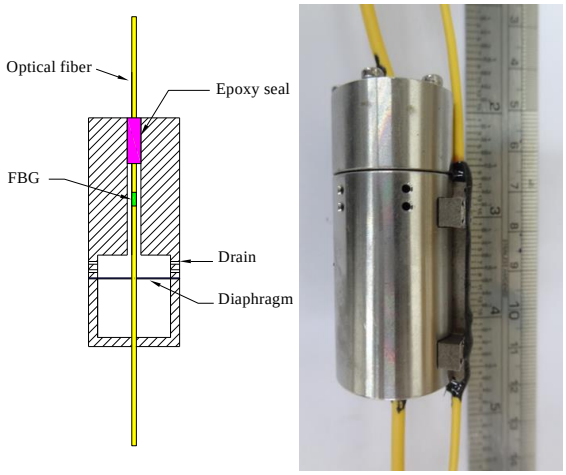

Figure 3 The FBG pressure transducer.

2.3 The FBG Extensometer

The FBG extensometer as shown in Figue 4 was developed to measure linear extension or compression. The linear movement induces relative motion between a roller and a wedge that in turn creates bending to a spring leaf. A pair of FBG attached to the spring leaf was used to measure bending of the spring leaf, where the amount of linear displacement was deduced from. Two pairs of spring leafs, separated by 180 degree were used for extension and compression measurement. The device was built to have a linear resolution of 8 μm, and a full range of 100mm in compression and 50mm in extension.

3. SLOPE STABILITY MONITORING AT FIVE TURN POINT

A section of Highway 18, referred to as the Five Turn Point has been selected as the most dangerous highway in Southern Taiwan. The slope area was approximately 1200m by 1000m where the ground surface elevation changed by as much as 400m (see Figure 5). At least eight sectors (designated as N1 to N8 in Figure 5) have been identified with either previous slope failure or signs of continuous movement. Figure 6 depicts cross sectional view of section B-B that has an average slope angle of 23˚. The shear planes associated with earlier ground failures according to available investigations are also included in Figure 6. Subsurface explorations revealed that the subject area was covered by 0-26m of colluvial material underlain by interlayered fractured sandstone and shale extended from below the colluvial to over 200m (deepest bore hole available) below the ground surface. Because of the wide range in sizes of the fractured rock pieces, it was not possible to obtain good quality samples for laboratory shearing tests and to provide representative strength parameters. The groundwater could rise from its low level by more than 20m as a result of heavy rainfalls according to available open end piezometer data shown in Figure 6. The sudden and significant change in groundwater table is believed to be a major cause for the earlier slope failures in this area.

A 60m deep borehole marked as NCTU-03 in Figures 5 and 6 was used to install the FBG piezometer array. The FBG pressure transducer, used as a piezometer was fitted inside of a 28mm ID and 32mm OD PVC pipe. Small drainage holes were drilled in the PVC pipe and wrapped with non-woven geotextile in areas surrounding the piezometer to allow passage of water. The piezometer was epoxied and sealed at both ends in the PVC pipe to prevent seepage between piezometers from within the PVC pipe. The PVC pipe serves as a spacer and housing for the piezometers and optical fibre. Final assembly was made as the PVC pipe lowered into the borehole. A comparison between an array of FBG piezometers installed in a single borehole to the case of individual standpipes is depicted in Figure 7. An array of GFBG-IPI was also installed close to NCTU-03, at depths from 30 to 60m. All sensors were connected to an on-site computer using optical fiber cables for optical signal interrogation and data logging/ transmission. Field installation was completed in September, 2007.

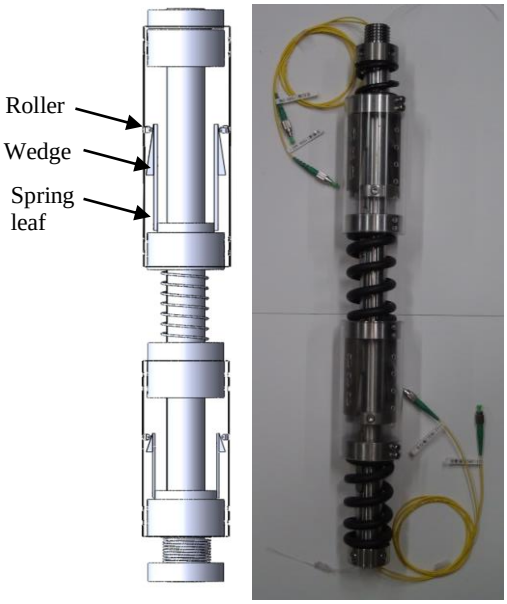

Figure 4 The FBG extensometer.

The Five Turn Point slope endured three major typhoons (i.e., Sinlaku of 2008, Morakot of 2009, and Fanapi of 2010) since September 2008, and remained stable till now (August, 2012). Of the three typhoon events, Morakot was the most damaging. A histogram of daily precipitations during typhoon Morakot at Five Turn Point is shown in Figure 8. Figure 9 shows a set of representative pressure head (h_p) profiles based on the FBG piezometer readings recorded from the beginning of typhoon Morakot to the time when h_p reached the maximum values.

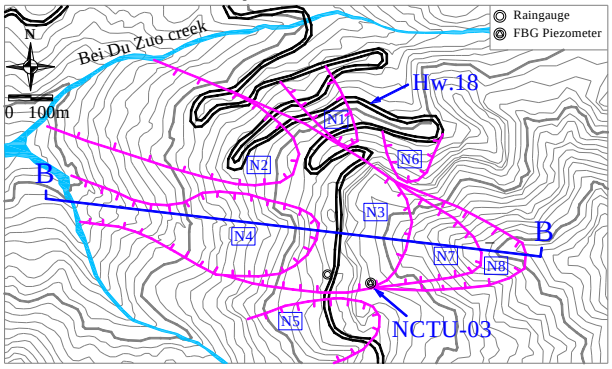

Figure 5. Topographic map of the Five Turn Point (after Land Engineering Consultants, Co., Ltd., 2007)

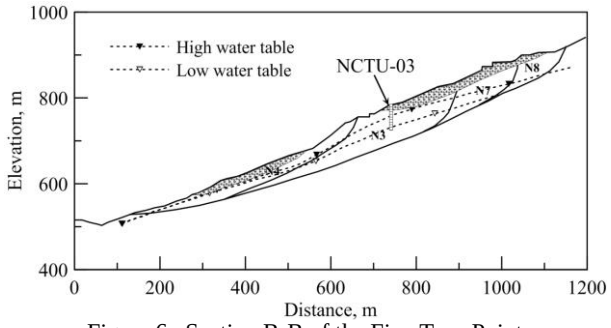

Figure 6. Section B-B of the Five Turn Point (after Land Engineering Consultants, Co., Ltd., 2007)

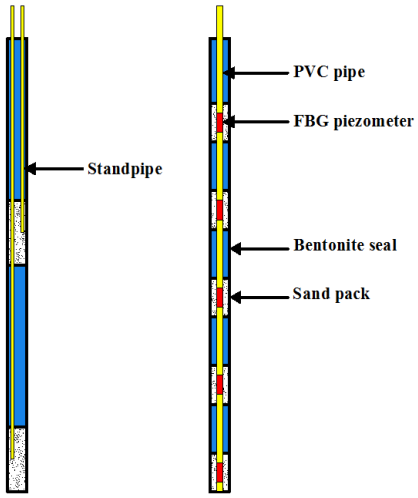

Figure 7 Comparison between the individual separate and piezometer array installations

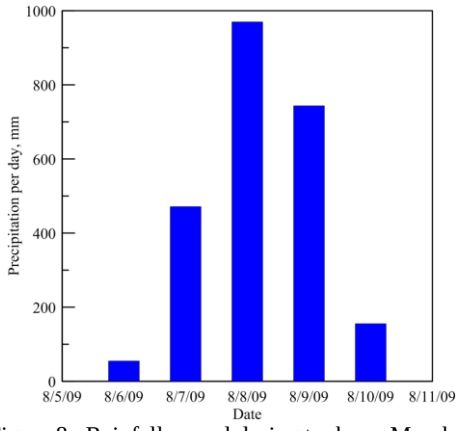

Figure 8. Rainfall record during typhoon Morakot

The pore-water pressure readings enabled the concept of field stress path (Anderson and Sitar, 1995; and Cascini et al., 2010) to be used in evaluating the stability of a slope. The initial state of stress at each of the pore-water pressure measurement locations was computed using the commercial software SIGMA/W (GEO-SLOPE, 2007). The computation was based on the cross section shown in Figure 6. The ground material was assumed to be linear elastic with Young's modulus E = 3310MPa, Poisson's ratio μ = 0.35, and total unit weight, $\gamma = 2\ \gamma_w$, where γ_w is the unit weight of water. For simplification, the single γ value used in the computation reflects a saturated state even when the material could be unsaturated. The potential error from this simplification is insignificant in comparison with the stress level and the effects of pore-water pressure variations (Anderson and Sitar, 1995). Considering a plane strain condition, the p (or p') and q were calculated as,

$$p' = (\sigma_1' + \sigma_2' + \sigma_3')/3 \qquad (1)$$

and

$$q = \frac{1}{\sqrt{2}}\sqrt{(\sigma_1' - \sigma_3')^2 + (\sigma_1' - \sigma_2')^2 + (\sigma_2' - \sigma_3')^2} \qquad (2)$$

where

σ_1', σ_2', and σ_3' = major, intermediate and minor principal stress, respectively

As the measured pore-water pressure increases, q at a given measurement point remained constant while p' decreases and the corresponding stress point (p', q) moves laterally towards a failure envelope as shown in Figure 9. The (p', q) points depicted in Figure 9 correspond to the respective nine FBG piezometer locations installed in the field. The lower left (p', q) points represent the state of field stress at shallower depths. The results also show a potential failure envelope that corresponds to a ϕ' close to 40°. Although not necessary for the Five Turn Point case, variations in slope angle and ground layers can be readily incorporated in the analysis under the framework of field stress path. It should be noted that the outcome of the linear elastic stress analysis was not sensitive to the selection of Young's modulus. However, the selection of Poisson's ratio could have significant effects on the initial p, q values.

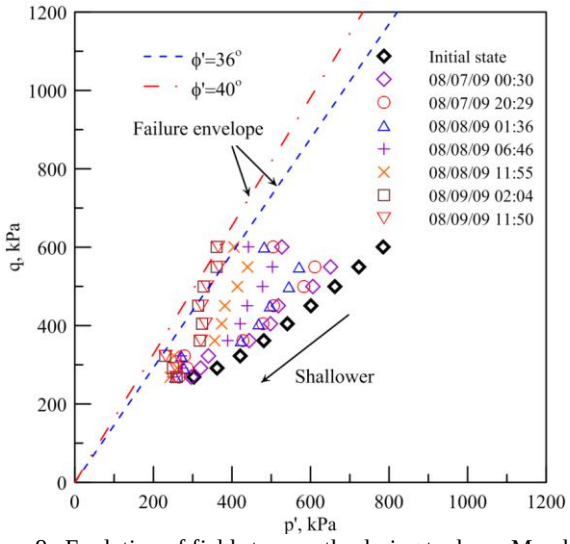

Figure 9. Evolution of field stress paths during typhoon Morakot.

4. GROUND SUBSIDENCE MONITORING AT GUAN-FU ELEMENTARY SCHOOL

Guan-Fu elementary school is located at the heart of an area in Central Western Taiwan, where the ground subsidence was the most, significant in the island. From 1999 to 2011, the accumulated subsidence was approximately 900mm. The soil alluvial soil deposit in this region is expected to be more than 1000m thick. Although, excessive ground water pumping is believed to the main reason for ground subsidence. The soil deposit was mostly granular with various amounts of fines (particles passing #200 sieve). It is thus difficult to attribute the settlement to soil consolidation typically occurs in cohesive soils. In order to ascertain the mechanisms of ground subsidence, the traditional magnetic rings and SONDEX sensor probe have been used to measure the ground settlement profile manually. Existing boreholes extending to a maximum depth of 300 m have been used for the purpose. Open-end piezometers, with a maximum number of 3, have been installed at selected depths to provide reference pore water pressure values. The metal tape and SONDEX measurement system had a resolution of 1 mm and repeatability of ±4 mm. Because of the deficiency in measurement resolution and miss-match between settlement and pore water pressure measurement depth frequencies, rigorous interpretation of the observed data has been difficult.

As a trial project, the authors installed a 100 m deep FBG ground subsidence monitoring array (schemetically shown in Figure 10) at the Guan-Fu elementary school test site. In this array, the FBG extensometers shown in Figure 4 were connected to a 10m long, 100 mm OD and 80 mm ID plastic pipes. The pipe was equipped with friction rings, spaced at 2 m to increase grip between the plastic pipe and the surrounding soil. An FBG piezometer was installed at the middle of each plastic pipe. Field installation of the FBG ground subsidence monitoring array (see Figure 10) was completely on April 26, 2012.

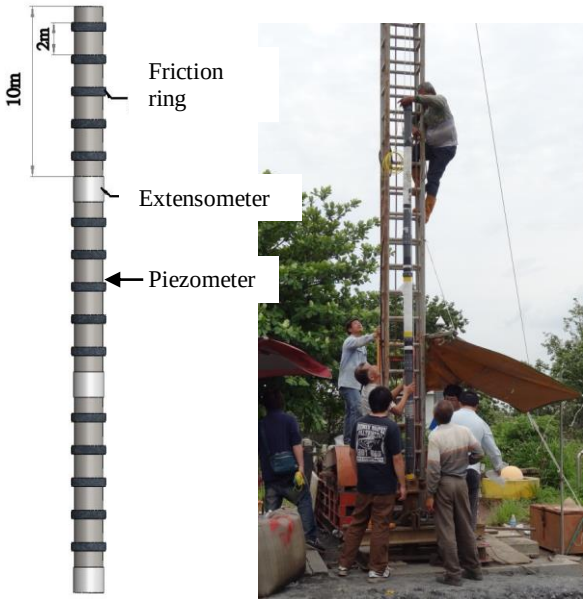

Figure 10 Field installation of the FBG ground subsidence monitoring array.

Figure 11 depicts the pore water pressure and ground settlement profiles according to the exiting readings at early stage following the field installation.

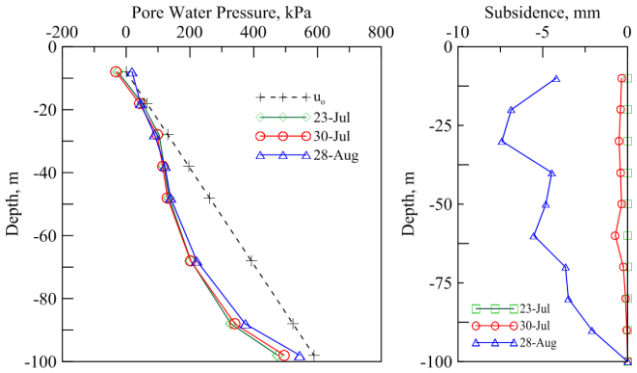

Figure 11 Pore water pressure and ground settlement profiles.

5. CONCLUDING REMARKS

The experience shows that with the help of partially distributive sensors, field pore-water pressure profile monitoring can be practically implemented. Taking advantage of the pore water pressure profile values, a stress based warning of a potential slope failure can be implemented. The stress based warning system considers the proximity between the current state of stress and failure envelope of the field material. We no longer rely solely on lateral displacement measurement as a means to project slope failure, as it has typically been done before.

The integrated, simultaneous pore water pressure and ground subsidence profile measurement provides real time data that can readily be used to analyze the potential mechanism or cause for ground subsidence.

6. REFERENCES

Anderson, S.A., and Sitar, N., 1995, "Analysis of rainfall-induced debris flows," Journal of Geotechnical Engineering, ASCE, 121(7), 544-552.

Cascini, L., Cuomo, S., Pastor, M., and Sorbino, G., 2010, "Modeling of Rainfall-Induced Shallow Landslides of the Flow-Type," Journal of Geotechnical and Geoenvironmental Engineering, 136(1), 85-98.

GEO-SLOPE International Ltd., 2007. ''SIGMA/W for stress-deformation.'' Version 7.17, User's guide, Geoslope Int. Lad., Calgary, Alta., Canada.

Kersey, A.D. 1992, "Multiplexed Fiber Optic Sensors." Fiber Optic Sensors, Proceedings of SPIE, Vol. CR44, pp.200-225.

Land Engineering Consultants, Co., Ltd. 2007, "Highway 28.9K~31.5K（Five Turn Point）landslide investigation, remediation planning and safety evaluation, 3rd overall report." Department of Highway Maintenance, Section V (in Chinese).

Meltz, G., Morey, W.W., and Glenn, W.H. 1989, "Formation of Bragg Gratings in Optical Fibers by a Transverse Holographic Methods." Optics Letters. Vol. 14, pp.283.

Rao, Y.J., 1998, "Fiber Bragg Grating Sensors: Principles and Applications," Optic Fiber Sensor Technology, Edited by K.T.V. Gattan and B.T. Meggitt, Published by Chapman and Hall, London, Vol. 2, 355-379.